On-Surface Synthesis of Ethynylene-Bridged Anthracene Polymers

Ana Sánchez-Grande, Bruno de la Torre, José Santos, Borja Cirera, Koen Lauwaet, Taras Chutora, Shayan Edalatmanesh, Pingo Mutombo, Johanna Rosen, Radek Zbořil, Rodolfo Miranda, Jonas Björk,* Pavel Jelínek,* Nazario Martín,* and David Écija*

Abstract: *Engineering low-band-gap π-conjugated polymers is a growing area in basic and applied research. The main synthetic challenge lies in the solubility of the starting materials, which precludes advancements in the field. Here, we report an on-surface synthesis protocol to overcome such difficulties and produce poly(p-anthracene ethynylene) molecular wires on Au(111). To this aim, a quinoid anthracene precursor with =CBr₂ moieties is deposited and annealed to 400 K, resulting in anthracene-based polymers. High-resolution nc-AFM measurements confirm the nature of the ethynylene-bridge bond between the anthracene moieties. Theoretical simulations illustrate the mechanism of the chemical reaction, highlighting three major steps: dehalogenation, diffusion of surface-stabilized carbenes, and homocoupling, which enables the formation of an ethynylene bridge. Our results introduce a novel chemical protocol to design π-conjugated polymers based on oligoacene precursors and pave new avenues for advancing the emerging field of on-surface synthesis.*

The design and study of π-conjugated polymers has received great attention during the last decades due to the relevant optical and electronic properties that emerge from the delocalization of the π-electrons. Such materials find use in different applications including light-emitting devices, solar cells, organic field-effect transistors, photocatalysis, and biosensors.[1–3] However, despite great synthetic advances in the field, there are enormous efforts coming from emerging areas of chemistry targeting to overcome the accompanying limitation of solubility, which precludes highly interesting conjugated nanomaterials to be synthesized by wet chemistry.[2,3]

On-surface synthesis has become a powerful discipline to design many novel molecular compounds, polymers, and nanomaterials with atomistic precision,[4–12] some of them not accessible by standard synthetic methods. Additionally, on-surface chemistry enables the structural and electronic characterization of the designed products with advanced surface-science techniques.[10,13,14] Recently, and within the scope of on-surface synthesis, particular success has been achieved in the field of oligoacenes, where anthracene,[15,16] tetracene,[17] hexacene,[18] heptacene,[19,20] nonacene,[21] decacene,[22] and undecacene[20] precursors have been deposited on coinage metals and transformed into oligoacene derivatives through external stimuli. However, despite the great potential of such acene compounds for plastic optoelectronics, the design of high-quality π-conjugated polymers exclusively based on oligoacene building units remains difficult. On-surface chemistry opens the gate to obtain acene-based polymers. Although their predicted intrinsic insolubility may hinder their practical application at first glance, state-of-the-art substrate-to-substrate transfer techniques already permit the implementation of highly insoluble nanomaterials into molecular electronic devices.[23]

Here, we report a comprehensive scanning tunneling microscopy (STM), non-contact atomic force microscopy (nc-AFM), and density functional theory (DFT) study of the on-surface synthesis of poly(p-anthracene ethynylene) molecular wires on Au(111). Our novel chemical approach is based on

[*] A. Sánchez-Grande, Dr. J. Santos, Dr. B. Cirera, K. Lauwaet, Prof. R. Miranda, Prof. N. Martín, Prof. D. Écija
IMDEA Nanociencia, C/ Faraday 9
Ciudad Universitaria de Cantoblanco
28049 Madrid (Spain)
E-mail: nazmar@quim.ucm.es
david.ecija@imdea.org

Dr. B. de la Torre, T. Chutora, Prof. R. Zbořil, Dr. P. Jelínek
Regional Centre of Advanced Technologies and Materials
Palacký University Olomouc
Šlechtitelů 27, 78371 Olomouc (Czech Republic)

Dr. B. de la Torre, S. Edalatmanesh, P. Mutombo, Dr. P. Jelínek
Institute of Physics, The Czech Academy of Sciences
Cukrovarnická 10, 16200 Prague 6 (Czech Republic)
E-mail: jelinekp@fzu.cz

Prof. J. Rosen, Dr. J. Björk
Department of Physics, Chemistry and Biology, IFM
Linköping University
58183 Linköping (Sweden)
E-mail: jonas.bjork@liu.se

Prof. R. Miranda
Departamento de Física de la Materia Condensada
Facultad de Ciencias, Universidad Autónoma de Madrid
28049 Madrid (Spain)

Prof. N. Martín
Departamento de Química Orgánica
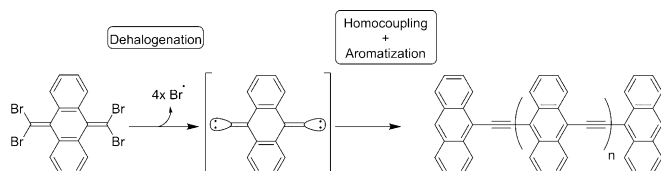Facultad de Ciencias Químicas, Universidad Complutense
28040 Madrid (Spain)

Supporting information and the ORCID identification number(s) for the author(s) of this article can be found under:
https://doi.org/10.1002/anie.201814154.

the dehalogenation, homocoupling, and aromatization of a quinoid anthracene precursor endowed with $=CBr_2$ moieties at their 9- and 10- positions. The deposition of this precursor (11,11,12,12-tetrabromoanthraquinodimethane), abbreviated **4BrAn**, on Au(111) gives rise to a close-packed assembly. Annealing to 400 K enables debromination, and, after diffusion, long molecular wires based on ethynylene bridges are formed, which is unambiguously confirmed by the excellent agreement of the experimental non-contact atomic force microscopy measurements with the theoretical simulations. A final step of annealing to 500 K induces the removal of peripheral bromine atoms and the subsequent emergence of isolated, high-quality, robust, and long anthracene-based polymers. Scanning probe microscopy reveals the shape and energy of the frontier orbitals, which leads to a band gap of 1.5 eV. The theoretical study of the reaction pathways, complemented by high-resolution scanning probe microscopy measurements with a CO tip, illustrates that the homocoupling process is based on an efficient dehalogenation of the molecular precursors and diffusion of the surface-stabilized carbenes, finally leading to coupling and aromatization of the polymeric chain.

Our study introduces a novel strategy to homocouple anthracene precursors, which could be extended to the whole family of oligoacenes. We envision that these results will notably contribute to the development of the field of on-surface chemistry while providing novel avenues to design π-conjugated polymers in the form of molecular chains, with a special emphasis in low-band gap nanomaterials.

Scheme 1 illustrates the suitably synthesized molecular precursor **4BrAn** used for building up the desired anthracene-based polymers. Notably, it incorporates $=CBr_2$ moieties at the positions 9 and 10 of the anthraquinone backbone to

Figure 1. a) Large-scale STM image of the parallelly aligned ethynylene-linked anthracene polymers coexisting with bromine atoms after deposition of a submonolayer coverage of **4BrAn** on Au(111) and subsequent annealing at 400 K ($V_{bias} = 100$ mV, $I = 10$ pA, image size $= 14.9 \times 8.4$ nm^2). b) Magnified constant-height nc-AFM and c) STM image (size $= 3.6 \times 3.2$ nm^2) of a selected area of (a) acquired at the same time. d) Chemical structure of an ethynylene-bridged anthracene moiety. e) Constant-height STM and f) nc-AFM image resolving the ethylene bond, which matches very well with g) a nc-AFM simulation (1.3×1.3 nm^2). h) Constant-height nc-AFM image of a linear (size $= 12 \times 2$ nm^2) and i) a curved (size $= 12 \times 4$ nm^2) ethynylene-linked anthracene polymer after annealing (a) to 500 K.

Scheme 1. Reaction sequence of the **4BrAn** (11,11,12,12-tetrabromoanthraquinodimethane) precursor after deposition on Au(111) and subsequent annealing.

control the dehalogenation and subsequent homocoupling upon thermal annealing[24] by undergoing an unprecedented reaction pathway as detailed below. The deposition of a submonolayer coverage of **4BrAn** on Au(111) results in the formation of close-packed islands in a rectangular unit cell (Supporting Information, Figure SI1). At this stage of the reaction, no isolated bromine atoms are detected on the surface, which highlights the integrity of the molecular precursors. A first step of annealing to 400 K leads to the emergence of long polymeric wires (Figure 1a and Supporting Information, Figure SI2). The molecular precursors have now lost their bromine atoms, which can be found either forming 1D atomic chains on the surface or located in between the polymers, directing their parallel alignment (Figure 1a and
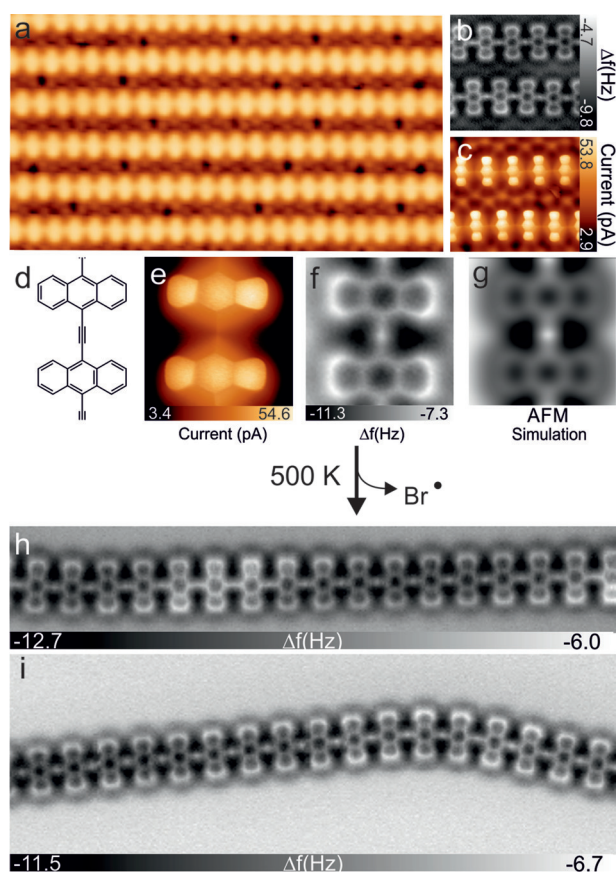
Supporting Information, Figure SI2). As illustrated by high-resolution AFM imaging with a CO tip, the polymers are formed by anthracene moieties that are linked by ethynylene bridges. At an adequate distance between tip and sample, the triple bond can be unambiguously distinguished as a bright protrusion (Figure 1b,f and Supporting Information, Figure SI3), which is in agreement with recently synthesized poly(*p*-phenylene ethynylene) molecular wires on Au(111).[25] The excellent match between the experimental and simulated AFM images confirms the bridge as an ethynylene moiety (see Figure 1f,g), which differs from the previously reported formation of cumulene bridges by dehalogenative homocoupling of alkenyl gem-dibromides.[24]

At this step of annealing, a small fraction of ethynylene-bridged anthracene dimers and trimers is present. High-resolution AFM resolves the conformation of these oligomers (Supporting Information, Figure SI4). The dimers are not planar due to the presence of terminal C atoms of the $=CBr_2$

moiety at each terminus of the dimer, which strongly interact with the substrate. This assumption is confirmed by the excellent agreement between the experimental and the simulated images. Notably, the trimer features a planar central anthracene, whereas the two terminal moieties are bent due to the interaction of the carbon termini with the gold support. Statistically, 90% of the molecular precursors are incorporated into the polymeric wires after a typical annealing of 30 min at 400 K. The edge of these wires always has the same C termination, resulting in terminal anthracene moieties that are bent towards the surface (Supporting Information, Figure SI4).

Importantly, the dehalogenated species diffuse as surface-stabilized carbenes until they connect and form the ethynylene-bridged anthracene polymers. This behavior is also typically encountered in the homocoupling of aryl halides on Au(111).[24–27] It is worth to highlight that the formation of anthracene polymers results in the aromatization of the quinoid precursors, since ethynylene bridges are preferred over cumulene bridges, regardless of the length of the polymer. The pro-aromatic nature of the quinoid precursor seems to be the driving force leading to the aromatization of the anthraquinoid core through electronic rearrangement. This scenario is fully supported by DFT calculations of the total energy, which also reveal the presence of the ethynylene bridges. The optimized structure of the polymer is almost planar, located 3.4 Å above the Au(111) substrate, and dominantly bonded by dispersion forces.

Further annealing of the sample to 500 K enables the desorption of the remaining bromine atoms, giving rise to isolated, long, and very high-quality ethynylene-bridged anthracene polymers (Figure 1h and Supporting Information, Figure SI5). Notably, the wires exhibit a remarkable degree of flexibility, allowing open curvatures up to 130° through minor bending of the ethynylene links (see Figure 1i). Additionally, the bond is robust and withstands tip-induced lateral manipulations, which results in a change in curvature of the polymer while preserving its chemical structure (Supporting Information, Figure SI6), thus indicating promising prospects for flexible electronics.

At this stage of annealing, the major termini of the polymers have lost the remaining carbon and are passivated by residual atomic hydrogen, as illustrated in Figures SI7 and SI8 (Supporting Information). Defects within the molecular chain are rare and structurally perfect ethynylene-bridged anthracene polymers with a length up to 30 nm are frequently observed.

To elucidate the electronic structure of the π-conjugated polymers, we simulated a freestanding polymer using the B3LYP density functional (Figure 2a), which reveals the presence of dispersive valence (VB) and conduction (CB) bands separated by a band gap of about 1.4 eV. The calculated projected density of states of the polymer on Au(111) indicates that the dispersion of both the CB and the VB remains practically unaltered with only a slight reduction of the band gap due to additional electron screening from the metal substrate (Supporting Information, Figure SI9).

Spatially resolved scanning tunneling spectra were recorded over the molecular wires and the clean Au(111)
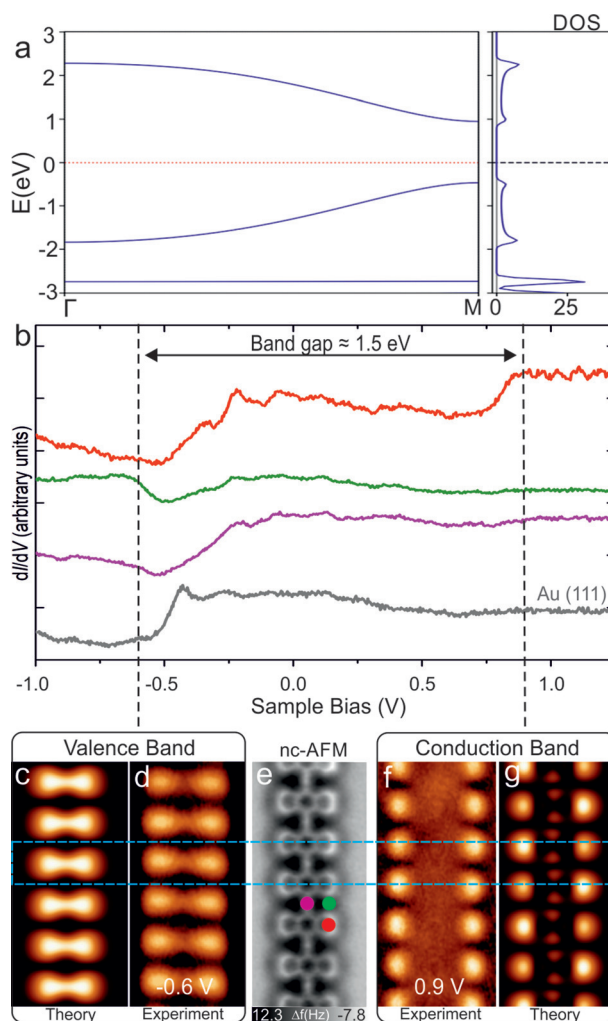

Figure 2. a) Calculated (B3LYP) electronic structure of a free-standing ethynylene-linked anthracene polymer. b) dI/dV scanning tunneling spectra of the polymer on Au(111) at selected points indicated by the colored dots in (e). c) Simulated STM image of the valence band. d) Experimental dI/dV map of the valence band at constant current. e) nc-AFM image of an ethynylene-linked anthracene polymer (size = 1.9 × 4.3 nm²). f) Experimental dI/dV map of the conduction band at constant current. g) Simulated STM image of the conduction band.

surface. As illustrated in Figure 2b, two frontier resonances can be distinguished at −0.6 eV (green curve) and 0.9 eV (red curve), which are tentatively assigned to the VB and CB edges, respectively. Note that the VB and CB edges are not located at the same position in space; the VB edge appears in between the anthracene moieties and the CB edge on top of them. Within the band gap, the downshifted surface state convoluted with tip states is observed. In agreement with the point spectra, the dI/dV map at the VB edge (Figure 2d) does not show maxima over the anthracene moieties, but shows states over the bridges and, remarkably, also on the voids adjacent to the links. The dI/dV map of the CB, on the contrary, shows states located over the edges of the anthracene moieties (Figure 2f). The calculated dI/dV maps (Figure 2c,g) match very well with the experiment, validating the

character of the band structure predicted by the DFT calculations. Analysis of the experimental STS spectra reveals a band gap of 1.5 eV. The polymer thereby shows a band gap circa 2 eV smaller than the 3.6 eV value recently reported for the HOMO–LUMO gap of a pure anthracene monomer on Au(111).[28] Notably, our results highlight the versatility of on-surface synthesis for designing polymers with varied band gaps going from large values in the case of poly(*meta*-phenylene)-like (3.7 eV)[29] or poly(*para*-phenylene) (3.2 eV)[30] polymers to small quantities (1.5 eV) as reported here.

Finally, we studied the reaction pathway for the homo-coupling of **4BrAn** on Au(111) with DFT-based transition state theory. The most favorable mechanism in which complete dehalogenation of the molecule initiates the reaction is shown in Figure 3. An alternative reaction pathway is
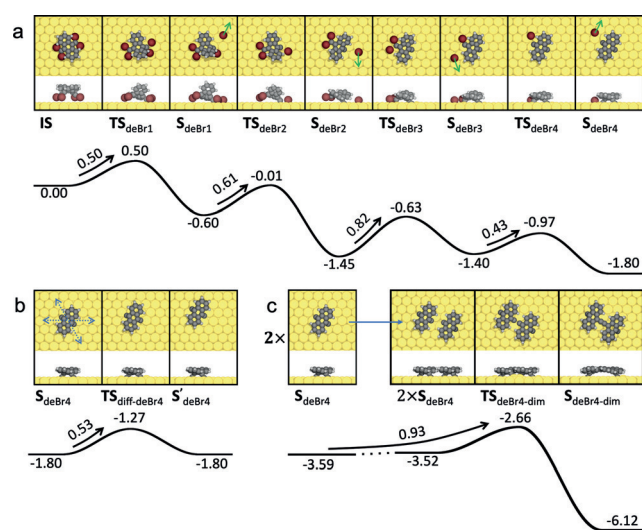

Figure 3. a–c) Energetically most favorable reaction pathway for the dehalogenative homocoupling of **4BrAn** precursors on Au(111), depicting top and side views of local minima ($\mathbf{S}_x$) and transition states ($\mathbf{TS}_x$) with the corresponding energy profile with respect to the initial state (**IS**): (a) Initial dehalogenation cascade, (b) diffusion of the dehalogenated molecule, and (c) coupling of two dehalogenated molecules. Energies in eV.

illustrated in Figure SI10 (Supporting Information) and discarded due to higher activation barriers. Removal of the third bromine has the highest activation energy (0.82 eV) and the full dehalogenation is highly exothermic with a reaction energy of −1.80 eV. The dehalogenated species ($\mathbf{S}_{deBr4}$) can then diffuse along two of the main directions of the substrate (Figure 3b) with a barrier of 0.53 eV. Finally, the activation energy for two molecules to approach each other and couple (Figure 3c) is 0.93 eV, similar to the dehalogenation step with the highest barrier. The coupling is a second-order process and one may expect the occurrence of non-coupled $\mathbf{S}_{deBr4}$ species. However, this would require sufficient time for a thermal equilibration of $\mathbf{S}_{deBr4}$ while avoiding coupling, that is, the excess heat released during dehalogenation could explain the absence of monomers following the initial annealing. Notably, the coupling between two molecules is

highly exothermic, as expected for the linking between two surface-stabilized carbenes.[26]

In conclusion, we report a strategy for the on-surface synthesis of ethynylene-bridged anthracene π-conjugated polymers. To this aim, we rely on the combination of scanning tunneling microscopy and non-contact atomic force microscopy complemented with state-of-the-art density functional theory. The deposition of quinoid moieties functionalized with =CBr₂ termini on Au(111) and subsequent annealing enable a unique reaction pathway. A first annealing step to 400 K results in the detachment of the bromine atoms and the diffusion of the resulting surface-stabilized carbenes until they couple, forming high-quality 1D molecular wires. Non-contact atomic force microscopy combined with simulations elucidates the structure of these ribbons as unprecedented ethynylene-bridged anthracene polymers. A second annealing step to 500 K enables the desorption of bromine, giving rise to long flexible polymers that preserve the integrity of the ethynylene bridge. These polymers exhibit a low experimental band gap of 1.5 eV, which is of potential relevance for near-infrared applications.

Importantly, preliminar results on Ag(111) also reveal the formation of ethynylene-linked anthracene polymers, thus expanding the scope of the reported reaction to other surfaces. Our results herald novel pathways to engineer π-conjugated polymers on surfaces, addressing the relevant family of acenes and thus contributing to the development of the field of on-surface chemistry and guiding the design of modern low-band-gap polymers.

Acknowledgements

Conflict of interest

The authors declare no conflict of interest.

[1] A. J. Heeger, *Angew. Chem. Int. Ed.* **2001**, *40*, 2591–2611; *Angew. Chem.* **2001**, *113*, 2660–2682.

[2] X. Guo, M. Baumgarten, K. Müllen, *Prog. Polym. Sci.* **2013**, *38*, 1832–1908.

[3] A. Facchetti, *Chem. Mater.* **2011**, *23*, 733–758.

[4] L. Grill, M. Dyer, L. Lafferentz, M. Persson, M. V. Peters, S. Hecht, *Nat. Nanotechnol.* **2007**, *2*, 687–691.

[5] J. Cai, P. Ruffieux, R. Jaafar, M. Bieri, T. Braun, S. Blankenburg, M. Muoth, A. P. Seitsonen, M. Saleh, X. Feng, et al., *Nature* **2010**, *466*, 470–473.

[6] A. Wiengarten, K. Seufert, W. Auwärter, D. Ecija, K. Diller, F. Allegretti, F. Bischoff, S. Fischer, D. A. Duncan, A. C. Papageorgiou, et al., *J. Am. Chem. Soc.* **2014**, *136*, 9346–9354.

[7] Q. Fan, J. M. Gottfried, J. Zhu, *Acc. Chem. Res.* **2015**, *48*, 2484–2494.

[8] L. Talirz, P. Ruffieux, R. Fasel, *Adv. Mater.* **2016**, *28*, 6222–6231.

[9] Q. Shen, H.-Y. Gao, H. Fuchs, *Nano Today* **2017**, *13*, 77–96.

[10] F. Klappenberger, Y.-Q. Zhang, J. Björk, S. Klyatskaya, M. Ruben, J. V. Barth, *Acc. Chem. Res.* **2015**, *48*, 2140–2150.

[11] B. Cirera, N. Gimenez-Agullo, J. Bjork, F. Martinez-Pena, A. Martin-Jimenez, J. Rodriguez-Fernandez, A. M. Pizarro, R. Otero, J. M. Gallego, P. Ballester, et al., *Nat. Commun.* **2016**, *7*, 11002.

[12] Q. Sun, R. Zhang, J. Qiu, R. Liu, W. Xu, *Adv. Mater.* **2018**, *30*, 1705630.

[13] T. Tseng, C. Urban, Y. Wang, R. Otero, S. L. Tait, M. Alcami, D. Ecija, M. Trelka, J. M. Gallego, N. Lin, et al., *Nat. Chem.* **2010**, *2*, 374–379.

[14] L. Gross, B. Schuler, N. Pavliček, S. Fatayer, Z. Majzik, N. Moll, D. Peña, G. Meyer, *Angew. Chem. Int. Ed.* **2018**, *57*, 3888–3908; *Angew. Chem.* **2018**, *130*, 3950–3972.

[15] J. Krüger, F. Eisenhut, T. Lehmann, J. M. Alonso, J. Meyer, D. Skidin, R. Ohmann, D. A. Ryndyk, D. Pérez, E. Guitián, et al., *J. Phys. Chem. C* **2017**, *121*, 20353–20358.

[16] S. Kawai, O. Krejčí, A. S. Foster, R. Pawlak, F. Xu, L. Peng, A. Orita, E. Meyer, *ACS Nano* **2018**, *12*, 8791–8797.

[17] J. Krüger, N. Pavliček, J. M. Alonso, D. Pérez, E. Guitián, T. Lehmann, G. Cuniberti, A. Gourdon, G. Meyer, L. Gross, et al., *ACS Nano* **2016**, *10*, 4538–4542.

[18] J. Krüger, F. Eisenhut, J. M. Alonso, T. Lehmann, E. Guitián, D. Pérez, D. Skidin, F. Gamaleja, D. A. Ryndyk, C. Joachim, et al., *Chem. Commun.* **2017**, *53*, 1583–1586.

[19] J. I. Urgel, H. Hayashi, M. Di Giovannantonio, C. A. Pignedoli, S. Mishra, O. Deniz, M. Yamashita, T. Dienel, P. Ruffieux, H. Yamada, et al., *J. Am. Chem. Soc.* **2017**, *139*, 11658–11661.

[20] R. Zuzak, R. Dorel, M. Kolmer, M. Szymonski, S. Godlewski, A. M. Echavarren, *Angew. Chem. Int. Ed.* **2018**, *57*, 10500–10505; *Angew. Chem.* **2018**, *130*, 10660–10665.

[21] R. Zuzak, R. Dorel, M. Krawiec, B. Such, M. Kolmer, M. Szymonski, A. M. Echavarren, S. Godlewski, *ACS Nano* **2017**, *11*, 9321–9329.

[22] J. Krüger, F. García, F. Eisenhut, D. Skidin, J. M. Alonso, E. Guitián, D. Pérez, G. Cuniberti, F. Moresco, D. Peña, *Angew. Chem. Int. Ed.* **2017**, *56*, 11945–11948; *Angew. Chem.* **2017**, *129*, 12107–12110.

[23] C. Moreno, M. Vilas-Varela, B. Kretz, A. Garcia-Lekue, M. V. Costache, M. Paradinas, M. Panighel, G. Ceballos, S. O. Valenzuela, D. Peña, et al., *Science* **2018**, *360*, 199.

[24] Q. Sun, B. V. Tran, L. Cai, H. Ma, X. Yu, C. Yuan, M. Stöhr, W. Xu, *Angew. Chem. Int. Ed.* **2017**, *56*, 12165–12169; *Angew. Chem.* **2017**, *129*, 12333–12337.

[25] Q. Sun, X. Yu, M. Bao, M. Liu, J. Pan, Z. Zha, L. Cai, H. Ma, C. Yuan, X. Qiu, et al., *Angew. Chem. Int. Ed.* **2018**, *57*, 4035–4038; *Angew. Chem.* **2018**, *130*, 4099–4102.

[26] J. Björk, F. Hanke, S. Stafström, *J. Am. Chem. Soc.* **2013**, *135*, 5768–5775.

[27] L. Dong, P. N. Liu, N. Lin, *Acc. Chem. Res.* **2015**, *48*, 2765–2774.

[28] J. Krüger, F. Eisenhut, D. Skidin, T. Lehmann, D. A. Ryndyk, G. Cuniberti, F. García, J. M. Alonso, E. Guitián, D. Pérez, et al., *ACS Nano* **2018**, *12*, 8506–8511.

[29] I. Piquero-Zulaica, A. Garcia-Lekue, L. Colazzo, C. K. Krug, M. S. G. Mohammed, Z. M. Abd El-Fattah, J. M. Gottfried, D. G. de Oteyza, J. E. Ortega, J. Lobo-Checa, *ACS Nano* **2018**, *12*, 10537–10544.

[30] N. Merino-Díez, A. Garcia-Lekue, E. Carbonell-Sanromà, J. Li, M. Corso, L. Colazzo, F. Sedona, D. Sánchez-Portal, J. I. Pascual, D. G. de Oteyza, *ACS Nano* **2017**, *11*, 11661–11668.